Received: 26 May 2021 | Revised: 7 July 2021 | Accepted: 14 July 2021

DOI: 10.1002/aoc.6389

RESEARCH ARTICLE

Applied Organometallic Chemistry WILEY

Continuous flow hydrogenation with Pd complexes of pyridine-benzotriazole ligands

Filiz Yılmaz | **Deniz Hür**

Faculty of Science Department of Chemistry, Yunusemre Campus, Eskisehir Technical University, Eskisehir, Turkey

Correspondence
Deniz Hür, Faculty of Science Department of Chemistry, Yunusemre Campus, Eskisehir Technical University, 26470 Tepebası, Eskisehir, Turkey.
Email: dhur@eskisehir.edu.tr

Funding information
Eskişehir Technical University, Grant/Award Number: 1701F025

Abstract

The use of continuous flow systems in chemical synthesis provides great advantages in terms of sustainability, efficiency, and safety. The ability to control reaction parameters such as temperature, pressure, and catalyst exposure in flow system enables rapid optimization of reaction conditions. In the present study, palladium complexes of 1-(piridin-2-il)-1*H*-benzo[*d*][1,2,3]triazol, *N*-((1*H*-benzo[*d*][1,2,3]triazol-1-il)metil)piridin-2-amin, and (1*H*-benzo[*d*][1,2,3]triazol-1-yl)(pyridin-2-yl)methanone ligands were synthesized and characterized. The catalytic activities of complexes are investigated in the hydrogenation of various alkenes such as styrene, cyclohexene, and 1-octene under continuous flow conditions. The complexes showed very high activity at 10-bar H_2 pressure and 50°C for short periods of 5–10 min. The catalysts reused for 10 cycles with no significant loss of catalytic activity.

KEYWORDS

benzotriazole, continuous flow, hydrogenation, palladium

1 | INTRODUCTION

Heterogeneous catalytic hydrogenation (HCH) has wide range application area[1–8] in different disciplines. Thus, synthesis of new and effective heterogeneous catalysts and efficiency investigation of these catalysts on various organic molecules by cheaper, environmentally compatible and rapid methods are among the issues that remain important today. From this perspective, organic conversion reactions carried out under continuous flow conditions have been become increasingly important in synthetic organic chemistry. Continuous flow processes provide significant advantages in terms of safety, efficiency, reproducibility, and waste reduction, as well as practical, efficient, and environmentally/sustainable organic transformations. Therefore, in recent years, continuous flow method has been an important tool for the efficiency and reusability of heterogeneous catalysts,[9–17] among many other synthetic organic applications.[18–22]

Recently, Yu et al. published a minreview[23] to evaluate innovations in continuous flow hydrogenation studies. In this study, recent studies on continuous flow homogeneous and heterogeneous catalysis of various organic functional groups such as alkenes and alkynes,[24–27] imines and nitro,[28,29] and carbonyl[30,31] were examined. Recent studies show that continuous flow hydrogenation has important advantages such as providing more effective control of reaction conditions, enabling industrial processes and laboratory-scale computer-controlled automatic experimentation, easy integration with instrumental analysis equipment such as FT-IR,[32] GC–MS, and benchtop NMR for faster analysis, safer hydrogen source usage, more effective catalyst-reactive interaction with good multiphase mixing, higher enantio-selectivity, higher reusability of catalysts, lower reaction temperature, and a shorter reaction time compared to batch processes. Benzotriazole is an important heterocyclic compound that can be

used in the development of new synthesis methods. It is resistant to many synthetic conditions, nontoxic, inexpensive, and easily removable in both acidic and basic medium.[33]

In this study, pyridine and benzotriazole ring containing ligands[33,34] and their palladium complexes have been synthesized. The catalytic activities of complexes have been investigated in hydrogenation of various alkenes in the continuous flow system. In catalytic experiments, temperature, H_2 pressure, and flow rate parameters were changed to determine optimum reaction conditions for each catalyst.

2 | EXPERIMENTAL

2.1 | Materials

All chemicals are used in analytical purity and purchased from Merck. FT-IR spectra were recorded between 400 and 4000 cm^{-1} using a Perkin Elmer Spectrum 100 Spectrometer. The samples were incorporated with KBr and pressed into a pellet. ^{1}H NMR spectra were measured on Agilent DDR2 400-MHz spectrometer using TMS as the internal standard. Thermogravimetric/differential thermal analyses were performed on a Perkin Elmer Diamond TG/DTA instrument. Hydrogenation reactions were performed with ThalesNano H-Cube®. The product distributions in the catalytic experiments were determined by Thermo Finnigan Trace GC including FID detector and Permabond column (SE-54-DF-0.25, 25 m × 0.32 mm i.d.).

2.2 | Synthesis

2.2.1 | Synthesis of 1-(piridin-2-il)-1*H*-benzo[*d*][1,2,3]triazol, **PyrBt**

PyrBt ligand was prepared by the methods reported in the literature.[35] 2-Bromopyridine (1 eq.) and 1*H*-benzotriazole (2 eq.) was refluxed in toluene for 24 h. After the reaction was completed, solvent was removed under vacuum, and the residue was dissolved in ethyl acetate, washed with saturated Na_2CO_3 to remove excess of benzotriazole. Obtained ^{1}H NMR and ^{13}C NMR results are identical with those in literature. Yield: 82%; FT-IR (KBr): ν 3110 (m), 3018 (m), 1590 (s), 1476 (s), 1441 (s), 1373 (w), 1285 (s), 1243 (w), 1065 (s), 758 (s) cm^{-1}; ^{1}H NMR (400 MHz, $CDCl_3$). δ = 8.66 (1H, d, J = 8.41 Hz), 8.62 (1H, dd, J = 4.87, 0.7 Hz), 8.31 (1H, d, J = 8.32 Hz), 8.13 (1H, d, J = 8.34 Hz), 7.95 (1H, dt, J = 8.46, 1.88 Hz), 7.61 (1H, dt, J = 8.09, 0.93 Hz), 7.46 (1H, dt, J = 8.13, 0.92 Hz), 7.33 (1H, ddd, J = 7.39, 4.88, 0.78 Hz) ppm; ^{13}C NMR for PyrBt (100 MHz, $CDCl_3$). δ = 114.8, 114.9, 120.0, 123.6, 125.8, 129.7, 131.3, 140.4, 146.5, 149.2, 151.2 ppm.

2.2.2 | Synthesis of *N*-((1*H*-benzo[*d*][1,2,3]triazol-1-il)metil)piridin-2-amin, **PyrNHCH$_2$Bt**

PyrNHCH2Bt ligand was prepared according to literature procedure.[36] The solution of 1*H*-benzotriazole (1 eq.) and 2-aminopyridine (1 eq.) in water was stirred for 5 min. Formaldehyde (37% w/w water, 1 eq.) was added dropwise to this mixture. The reaction mixture was stirred for 1 h. The precipitated solid is filtered and recrystallized from an ethyl acetate/hexane mixture to give the product. Yield: 76%; FT-IR (KBr): ν 3394 (s), 3093 (w), 3024 (m), 1610 (s), 1514 (s), 1453 (s), 1325 (s), 1296 (s), 1165 (s), 760 (s) cm^{-1}; ^{1}H NMR (400 MHz, $CDCl_3$). δ = 8.20 (1H, s), 8.03–7.94 (2H, m), 7.49–7.38 (2H, m), 7.33 (1H, t, J = 14.33, 7.29 Hz), 6.72–6.65 (1H, m), 6.52 (1H, d, J = 8.2 Hz), 6.36 (2H, d, J = 6.91 Hz), 5.66 (1H, s, br.) ppm; ^{13}C NMR (100 MHz, $CDCl_3$). δ = 54.0, 108.9, 111.2, 115.0, 119.5, 123.9, 127.3, 132.8, 137.8, 147.7, 155.9 ppm.

2.2.3 | Synthesis of (1*H*-benzo[*d*][1,2,3]triazol-1-yl)(pyridin-2-yl)methanone, **PyrCOBt**

PyrCOBt ligand was prepared according to literature.[37] A solution of 2-picolinic acid (1 eq.), mesitylbenzotriazole (1 eq.), and triethyl amine (2 eq.) in 20 ml of dry THF was dissolved in an 80-ml pressure tube under nitrogen atmosphere. The reaction mixture was kept under 80-W microwave irradiation for 1 h. When the reaction was completed, the solvent was evaporated under vacuum. The reaction mixture was dissolved in ethyl acetate and extracted with 20% Na_2CO_3 (aq) solution (5 × 20 ml). The organic phase was dried with sodium sulfate, and the solvent was evaporated under vacuum to give the product. Yield: 92%; FT-IR (KBr): ν 1706 (s), 1593 (m), 1484 (m), 1450 (m), 1367 (m), 1217 (s), 1045 (s), 742 (s) cm^{-1}; ^{1}H NMR (400 MHz, $CDCl_3$, TMS). δ = 8.81 (d, J = 4.64 Hz, 1H), 8.33 (d, J = 8.83 Hz, 1H), 8.11 (d, J = 7.68 Hz, 1H), 8.07 (d, J = 7.86 Hz, 1H), 7.91 (t, J = 7.78 Hz, 1H), 7.66 (t, J = 7.69 Hz, 1H), 7.56–7.48 (m, 2H) ppm; ^{13}C NMR (100 MHz, $CDCl_3$, TMS). δ = 114.5, 120.2, 125.7, 126.3, 126.5, 126.9, 130.5, 131.8, 136.7, 145.6, 149.8, 165.0 ppm.

2.2.4 | Synthesis of dichloro[1-(piridin-2-il)-1*H*-benzo[*d*][1,2,3]triazol]palladium(II), **PyrBt-Pd**

PyrBt ligand (1 eq.) was stirred with $PdCl_2$ (1 eq.) in acetonitrile at room temperature for 18 h. The yellow solid was isolated by filtration and dried under vacuum to give PyrBt-Pd complex (Scheme 1). Yield: 84%; FT-IR (KBr): ν 3113 (w), 1602 (m), 1473 (s), 1440 (m), 1309 (m), 1253 (w), 1174 (m), 766 (s) cm^{-1}; ^1H NMR (400 MHz, DMSO-d_6). $\delta = 8.68$ (1H, d, $J = 3.9$ Hz), 8.56 (1H, d, $J = 8.34$ Hz), 8.23 (1H, d, $J = 8.2$ Hz), 8.21–8.10 (2H, m), 7.70 (1H, t, $J = 15.04$, 7.39 Hz), 7.57–7.49 (2H, m) ppm. ^{13}C NMR (100 MHz, DMSO-d_6). $\delta = 114.8$, 114.9, 118.3, 120.0, 123.6, 125.8, 127.9, 129.6, 140.4, 149.2 ppm.

2.2.5 | Synthesis of dichloro[*N*-((1*H*-benzo[*d*][1,2,3]triazol-1-il)metil)piridin-2-amin] palladium(II), **PyrNHCH$_2$Bt-Pd**

Solution of $PdCl_2$ (1 eq.) in dry hot acetonitrile was added dropwise to solution of ligand $PyrNHCH_2Bt$ (1 eq.) in acetonitrile under nitrogen atmosphere. The reaction mixture was stirred 24 h at 60°C under nitrogen atmosphere. Dark yellow precipitate was filtered and washed with chloroform. Solid residue was dried under vacuum to give $PyrNHCH_2Bt$-Pd complex. Because the complex is insoluble in NMR solvents, its structure was determined using only the IR spectrum. Yield: 81%; FT-IR (KBr): ν 3445 (broad), 3333 (s), 1617 (s), 1576 (s), 1523 (s), 1452 (m), 1324 (s), 1270 (s), 1158 (s), 744 (s) cm^{-1}. ^1H NMR (400 MHz, DMSO-d_6). $\delta = 9.60$ (1H, s), 8.06 (d, $J = 8.22$ Hz, 2H), 7.76 (t, $J = 5.60$ Hz, 1H), 7.46–7.32 (m, 2H), 6.97 (s, 1H), 6.87 (d, $J = 8.38$ Hz, 1H), 6.62 (d, $J = 7.80$ Hz, 1H), 6.24 (d, $J = 7.67$ Hz, 1H), 5.32 (s, 1H) ppm. ^{13}C NMR (100 MHz, DMSO-d_6). $\delta = 65.0$, 111.3, 113.0, 114.9, 118.3, 119.3, 137.8, 139.6, 142.5, 148.4, 151.6, 156.2 ppm.

2.2.6 | Synthesis of dichloro[(1*H*-benzo[*d*][1,2,3]triazol-1-yl)(pyridin-2-yl)methanone] palladium(II), **PyrCOBt-Pd**

Solution of PyrCOBt (1 eq.) and $PdCl_2$ (1 eq.) in acetonitrile was refluxed 24 h. Yellow precipitates were filtered and dried under vacuum to obtain PyrCOBt-Pd complex. Yield: 85%; FT-IR (KBr): ν 3473 (broad), 3105 (s), 1753 (m), 1684 (s), 1608 (s), 1459 (s), 1336 (s), 1226 (s), 1157 (m), 1047 (m), 755 (s) cm^{-1}. Because of insolubility no NMR data were recorded.

2.3 | General catalytic hydrogenation procedure in continuous flow system

Hydrogenation reactions were performed with ThalesNano H-Cube® in Figure 1. The hydrogen gas produced by the H-Cube® system in high purity by electrolysis of water was directly supplied to the system at the desired pressure. The catalyst (3 mg), which was grounded together with silica (125 mg), was filled into the 5-cm-long cartridge and placed on the port in the system. The 0.1 M substrate solution in ethanol was loaded into the system with an HPLC pump. Reaction temperature and H_2 pressure were controlled through the system and adjusted to the determined values. The reaction residual time was determined as 5 min for 1 ml min^{-1} and 10 min for 0.5 ml min^{-1} in flow, respectively. The product distributions in the samples taken at the end of the reaction were determined by GC. After each catalytic reaction in the system, the pure solvent was passed over the cartridge to remove the substrate and product residues from the catalyst bed. To determine the ideal washing time, samples were taken from the system at certain times and analyzed with the GC. According to the GC analysis results, the ideal colon washing time was determined as 40 min in all experiments.

3 | RESULT AND DISCUSSION

3.1 | Characterization

3.1.1 | Characterization of PyrBt and PyrBt-Pd

In the ^1H NMR spectrum of PyrBt ligand, two doublet signals recorded at 8.66 and 8.31 ppm and two triplet signals recorded at 7.61 and 7.46 ppm are the signals of the characteristic Bt-1 isomer. The doublet of doublet recorded at 8.62 ppm, the doublet seen at 8.13 ppm, the doublet of triplet seen at 7.95 ppm, and the doublet of the doublet recorded at 7.33 ppm are the signals of 2-substituted pyridine. Although the ^1H NMR spectrum of the PyrBt-Pd complex contains the same signals as PyrBt as expected, shifts and widening of the peaks were observed due to metal binding (see Figures S1 and S2).

In the FT-IR spectrum of the ligand PyrBt (see Figure S5), aromatic CH stretching vibrations of benzotriazole and pyridine groups were recorded at 3110 cm^{-1} and 3018 cm^{-1}, aromatic CC + CN (benzotriazole) stress at 1590, 1476, and 1441 cm^{-}1. The C—N stretching of the pyridine ring was observed at 1373 and 1243 cm^{-1}, and the N═N strain of the benzotriazole ring

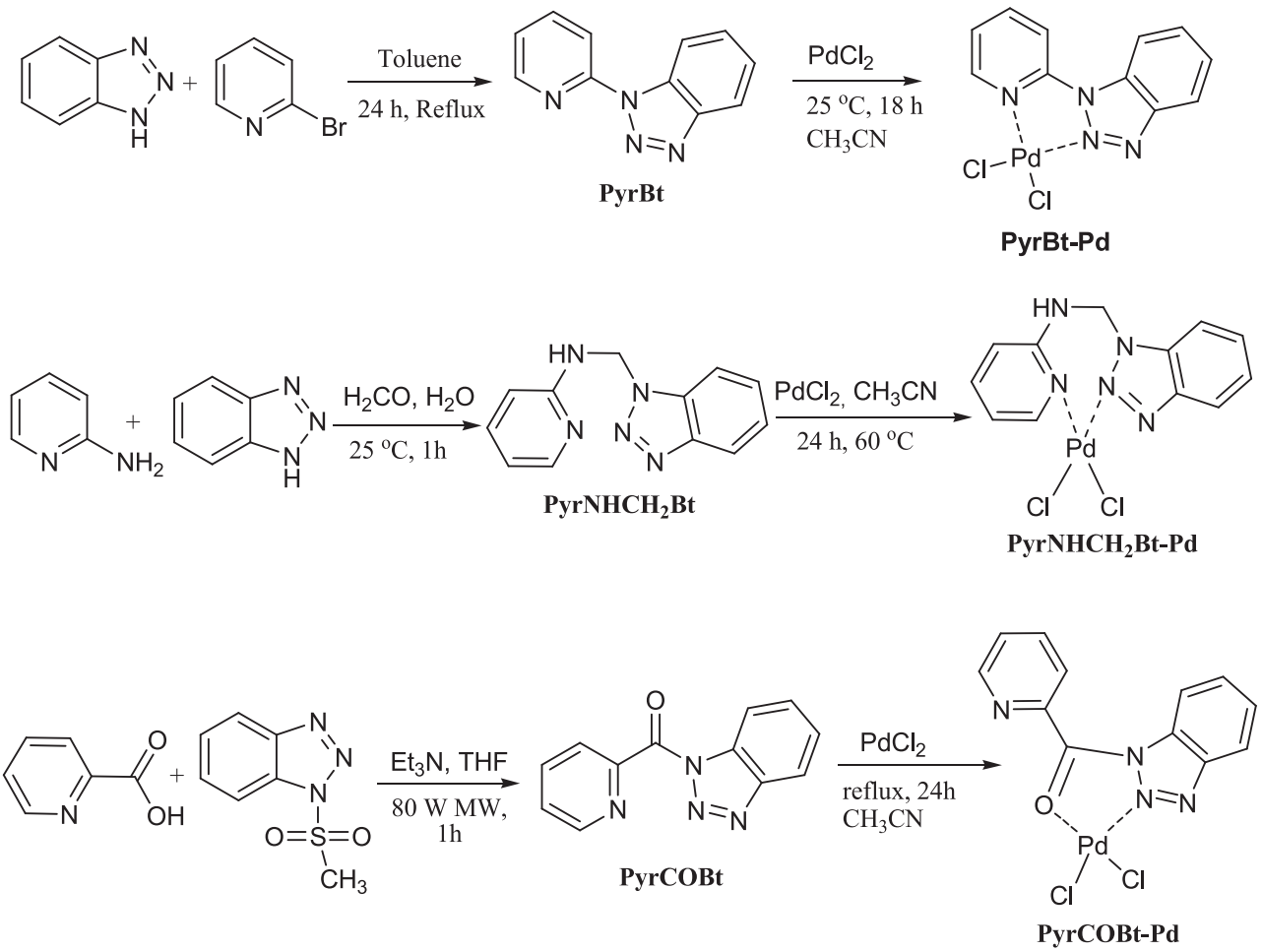

SCHEME 1 The schematic preparation of ligands and complexes (complex structures are proposed structures)

FIGURE 1 Flow system (H-Cube®) using catalytic experiments

was observed at 1285 cm^{-1}. The peaks observed at 1065 cm^{-1} belong to C—H bendings, while the strong peak observed at 758 cm^{-1} belongs to C—C bendings. In the FT-IR spectrum of the PyrBt-Pd complex (see Figure S6), it was observed that the vibration frequency of benzotriazole N=N stretching shifted from 1285 to 1253 cm^{-1} after coordination with metal. The reason for this 30-cm^{-1} frequency shift is that the coordination with the metal through nitrogen atoms reduces the electron density in the N=N bond. In addition, the fact that the value of the C—N (benzotrizale) stretching frequency, observed at 1441 cm^{-1}, does not change after the formation of the complex reduces the possibility of the benzotriazole ring coordinating with the metal over the N3 atom. If there is coordination from the N3 atom, there should be a decrease in triazole C—N vibrations. When the changes in the stress vibrations of the pyridine ring were examined, the C—N stretching vibrations observed at 1373 and 1243 cm^{-1} decreased to 1367 and 1204 cm^{-1} after the complex formation. This decrease in frequency indicates that the pyridine ring is in coordination with the metal. For this reason, it was thought that metal is bonded from benzotriazole to N2 nitrogen and pyridine nitrogen is likely to be formed. These results are

consistent with the results we obtained with spectroscopic and computational methods in our previous study.[38]

Thermal analysis (TG/DTA/DTG) of complexes was performed under N_2 atmosphere in the temperature range from ambient to 900°C. The TG/DTA/DTG curve of PyrBt-Pd complex is shown in Figure S7. The thermal dehydration takes place between 30°C and 192°C, with a mass loss 4.77% (calcd. 4.47). The thermal decomposition from 320°C to 410°C, with mass loss 44.47% (calcd. 45.29%) corresponds to the thermal decomposition of the $C_{11}H_9N_2$ fragment of PyrBt ligand. The maximum rate of mass loss is indicated by the DTG peak at 345.9°C. One endothermic peak with $t_{max} = 348.7$°C on the DTA curve was observed at this stage. The second decomposition process attributable to pyrolysis of the other fragments occurred at 400°C to 800°C with a mass loss 25.26%. Two exothermic peaks with $t_{max} = 427.2$°C and 781.8°C on the DTA curve were observed for this step. The overall mass losses are observed to be 75.99%, which is in very good agreement with the calculated value of 76.59%. The final residue, estimated as Pd^0, has the observed mass 24.01% as against the calculated value of 23.41%.

3.1.2 | Characterization of $PyrNHCH_2Bt$ and $PyrNHCH_2Bt$-Pd

The ^1H NMR spectrum of the $PyrNHCH_2Bt$ ligand has mixed cleavage signals. This result is consistent with the literature and the reason is that the free rotation of Bt-1 and

—NH— groups around —CH_2— bridge. The singlet signal seen at 8.20 ppm is the aromatic CH-proton neighboring to the pyridine nitrogen. The multiple signals seen at 8.03–7.94 ppm are benzene —CH protons of benzotriazole. On the other hand, the multiple peaks seen in the 7.49- to 7.38-ppm range are the overlapping signals of benzotriazole and pyridine protons. The characteristic methylene (—CH_2—) signal between —NH— and benzotriazole expected for this compound was recorded as a doublet signal by interacting with the NH proton at 6.36 ppm. In addition, the NH signal recorded at 5.66 ppm was recorded as a broad signal while waiting for a triplet, which is a result of the free rotational motion (see Figure S8). $PyrNHCH_2Bt$-Pd complex is slightly soluble in DMSO-d_6 even when irradiated with microwave. Some signal shifts and broadenings were recorded in ^1H NMR of this complex. Additionally, the CH signal adjacent to the pyridine nitrogen shifted to a significantly lower area than the same signal of the ligand. This supports the binding of the metal to the pyridine nitrogen. ^1H NMR and ^{13}C NMR of $PyrNHCH_2Bt$-Pd are given in Figures S11 and S12, respectively.

In the FT-IR spectrum of the ligand $PyrNHCH_2Bt$, C—H stretching vibrations of the benzotriazole ring are observed at 3394 and 3337 cm^{-1}, and the combination bands of C═N and N═N stretching are observed at 1514 cm^{-1}. The C—H vibrations of the pyridine ring of the ligand are 3093 and 3024 cm^{-1}, and the C═N tensile vibrations are 1610 cm^{-1} (see Figure S10) After coordination with the metal, the shift of C—N vibrations in both the pyridine ring and benzotriazole ring to high frequency (1617 and 1576 cm^{-1}) shows that the ligand coordinates with the metal through the nitrogen donor atoms in both the pyridine and benzotriazole ring. For this reason, it is thought that metal binding formed via pyridine nitrogen and N2— nitrogen of benzotriazole for the $PyrNHCH_2Bt$-Pd complex (see Figure S13).

The thermal decomposition of the $PyrNHCH_2$-Pd complex occurs in multiple stages (see Figure S14). The thermal dehydration of this complex takes place between 30°C and 192°C, with a mass loss of 4.77% (calcd. 4.47). The first decomposition process occurred in the temperature range 195°C to 320°C, with a mass loss of 18.39% (calcd 19.38). The DTA peak corresponding to this stage is a small endothermic peak at 258.5°C. The second decomposition between 320°C and 442°C with a mass loss of 22.21% may be attributed to the removal of benzotriazole part of ligand, and DTG peak corresponding to this stage is found at 406.2°C with a maximum rate of mass. An exothermic peak with $t_{max} = 417.9$°C on the DTA curve was observed for this step. The mass of the final residue corresponded to stable PdO, 28.91% (calcd. 30.4).

3.1.3 | Characterization of PyrCOBt and PyrCOBt-Pd

Characteristics of two doublet signals at around 8.10–8.30 ppm and two triplets at 7.60–7.79 ppm are recorded for *N*-acylbenzotriazole in ^1H NMR spectra. Additionally, disappearance of expected broad signal at around 10.0–12.0 ppm for hydroxy signal of 2-picolinic acid supports bonding of benzotriazole ring (see Figure S15). Unfortunately, no NMR spectra could be recorded for PyrCOBt-Pd complex, because it is not soluble in NMR solvents, such as DMSO-d_6, CD3OD, and DMF-d_7 solvents even under microwave irradiation.

When the FT-IR spectra of the ligand and the complex are compared, the shift of the carbonyl (C═O) stretching is observed. While C═O signal is recorded at 1706 cm^{-1} for PyrCOBt, after the complex formation, it

appeared at 1753 cm^{-1} (see Figures S17 and S18). The shifting of the C—N stretching vibrations of the benzotriazole ring from 1593 to 1608 cm^{-1} supports metal coordinate with carbonyl oxygen and N1 nitrogen in the benzotriazole ring.

The thermogram of PyrCOBt complex is shown in Figure S19. A mass loss of 2.26% between 35°C and 180°C is due to absorbed water. The second stage, which occurs in the temperature range of 180°C and 305°C, corresponds to the decomposition of an organic part of the ligand, with the DTG peak observed at 268.4°C (mass loss of 24.47%). The next step from 305°C to 440°C with a mass loss 23.37%, accompanied by an exothermic peak with t_{max} = 420.6°C on the DTA curve, may be attributed to the pyrolysis of ligands. DTG peak corresponding to this stage is found at 415.1°C with a maximum rate of mass. Total mass loss was observed as 73.55% (calcd. 73.49). The final residue, estimated as Pd^0, has the observed mass 26.45% as against the calculated value of 26.39%.

3.2 | Catalytic activity of palladium complexes in hydrogenation of various alkenes

The efficiency of the synthesized palladium complexes was tested in styrene, 1-octene, and cyclohexene hydrogenations. In the hydrogenation of styrene and cyclohexene, ethyl benzene and cyclohexane are formed, respectively. 1-Octene is selectively hydrogenated to *n*-octane, but some isomer products such as 2-octene and 3-octene may be formed during the hydrogenation (Scheme 2).

3.2.1 | Catalytic activity of PyrBt-Pd

Experiments in styrene hydrogenation were carried out at 25°C and 50°C. It was found that the increase in temperature had a positive effect on the effectiveness of PyrBt-Pd catalyst (Entries 1 and 2 in Table 1). On the contrary, the increase in H_2 pressure caused a small decrease in the activity of catalyst (Entries 2 and 3). This may be due to the catalyst being deactivated under high pressure. Best conversion (100%) in styrene hydrogenation was obtained at 50°C, 10-bar H_2 pressure, and 1-ml min^{-1} flow rate (TOF = 14,880). The substrate concentration is 0.1 M in the experiments carried out under these optimum conditions. By keeping these conditions constant, when the substrate concentration was increased to 0.5 M, the ethylbenzene conversion was found to be as 81.62% (Entry 4). Although the number of substrate molecules in the medium increased approximately five times, the product conversion over 80% indicates that the efficiency of PyrBt-Pd catalyst is very high. When flow rate reduced to 0.5 ml min^{-1}, the ethylbenzene conversion increased to 97.85% (Entry 5). At low flow rate,

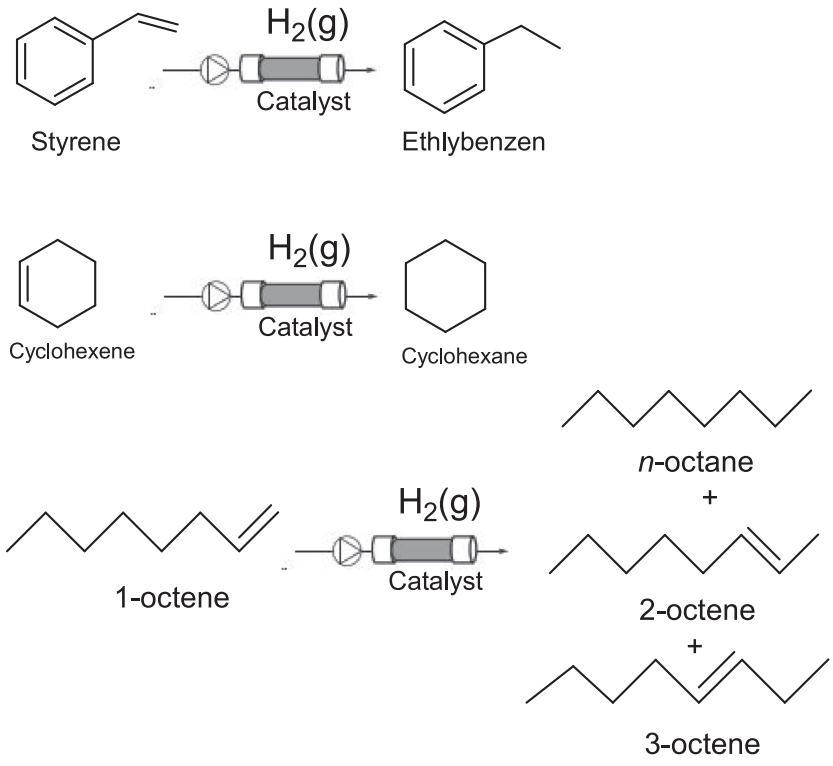

SCHEME 2 The catalytic hydrogenation of styrene, cyclohexene, and 1-octene in flow system using H-Cube®

TABLE 1 Catalytic activity of PyrBt-Pd complex

Substrate	Entry	*T* (°C)	$C_{subst.}$ (M)	Flow rate (ml min^{-1})	H_2 pres. (bar)	Total conv. (%)	Main product (Distrib.%)	TON	TOF
Styrene	1	25	0.1	1	10	68.91	Ethylbenzene	854	10,248
	2	50	0.1	1	10	100	Ethylbenzene	1240	14,880
	3	50	0.1	1	50	96.3	Ethylbenzene	1194	14,328
	4	50	0.5	1	10	81.62	Ethylbenzene	506	6072
	5	50	0.5	0.5	10	97.85	Ethylbenzene	607	3642
1-Octene	6	25	0.1	1	10	100	*n*-Octane (80.2%) 2-Octene (15.7%) 3-Octene (4.1%)	994	11,928
	7	50	0.1	1	10	100	*n*-Octane (83.0%) 2-Octene (13.2%) 3-Octene (3.8%)	1029	12,348
	8	50	0.1	0.5	10	100	*n*-Octane	1240	7440
	9	50	0.1	1	50	100	*n*-Octane	1240	14,880
	10	50	0.5	0.5	10	99.3	*n*-Octane (83.5%) 2-Octene (11.9%) 3-Octene (3.9%)	518	3108
Cyclohexene	11	25	0.1	1	10	40.8	Cyclohexane	506	6072
	12	50	0.1	1	10	49.5	Cyclohexane	614	7366
	13	50	0.1	0.5	10	82.5	Cyclohexane	1023	6138
	14	50	0.1	0.5	20	97.06	Cyclohexane	1204	7221
	15	50	0.1	0.5	30	99	Cyclohexane	1228	7366
	16	50	0.1	0.5	50	100	Cyclohexane	1240	7440
	17	50	0.5	0.5	50	95.46	Cyclohexane	592	3551

Note: Residual time is 10 and 5 min for 0.5- and 1-ml min^{-1} flow rates, respectively. $n_{subst} = 0.01$, $n_{cat.} = 8.0315 \times 10^{-6}$.

substrates residence time in the column increases, so they can interact with the catalyst for a longer time.

In hydrogenation of 1-octene at 25°C with the PyrBt-Pd complex, the total conversion reached 100%; but under these conditions, besides *n*-octane, other hydrogenation products, 2-octene and 3-octene, were also detected. The distributions of 2-octene and 3-octane were determined as 15.7% and 4.1%, respectively (Entry 6). Although the temperature increased to 50°C, the *n*-octane conversion increased from 80.2% to 83%, but isomers were still observed in the mixture (Entry 7). One hundred percent *n*-octane selectivity was achieved when the flow rate was reduced to 0.5 ml min^{-1} while keeping temperature and pressure constant (50°C, 10 bar, Entry 8). Another way to increase *n*-octane selectivity is by increasing the pressure of hydrogen gas. It was determined that 1-octene was converted to *n*-octane without any isomer formation at 50-bar H_2 pressure at a flow rate of 1 ml min^{-1} (Entry 9). The reaction time is shorter at a flow rate of 1 ml min^{-1}. The important point in catalytic reactions is to reach high TOF values. According to varying reaction parameters, the highest TOF value was reached in 1-octene hydrogenation at 50°C temperature, 50-bar H_2 pressure, and 1-ml min^{-1} flow rate. In order to examine the effect of the substrate concentration on the activity of the catalyst, the substrate concentration was increased from 0.1 to 0.5 M. As can be seen in Entries 8 and 10 in Table 1, the TOF value decreases more than half at 0.5 M concentration. This result is as expected due to the increasing number of substrate molecules in the mixture.

The efficiency of the PyrBt-Pd complex was also tested in hydrogenation of cyclohexene, a cyclic alkene. In cyclohexene hydrogenation, the reducing product is cyclohexane. In the experiments conducted at 25°C and 50°C (1-ml min^{-1} flow, 10-bar H_2), it was determined that the cyclohexane conversion was below 50% (Entries 11 and 12). When the flow rate was reduced to 0.5 ml min^{-1}, the conversion was increased to 82.5%. Therefore, the ideal column flow rate was set at 0.5 ml min^{-1}, and the H_2 gas pressure was gradually increased from 10 to 50 bar (Entries 13–16). It was

determined that there was an increase in cyclohexane conversion parallel to the increase in pressure. The highest TOF value was obtained at 0.5-ml min^{-1} flow rate, 50°C temperature, and 50-bar H_2 pressure (Entry 16).

3.2.2 | Catalytic activity of PyrNHCH$_2$Bt-Pd

The efficiency of PyrNHCH$_2$Bt-Pd complex in styrene hydrogenation was initially investigated at 25°C, 10-bar H_2 pressure, and 1-ml min^{-1} flow rate, and 21.3% ethylbenzene formation was determined under these conditions (Entry 1 in Table 2). Keeping the temperature constant and reducing the flow rate to 0.5 ml min^{-1} only provided a 1% increase in conversion (Entry 2). It was observed that the conversion of ethylbenzene increased to 50% when the temperature was increased to 50°C at flow rate of 1 ml min^{-1} (Entry 3). This result indicates that the temperature has a positive effect on the PyrNHCH$_2$Bt-Pd catalyst activity. In order to determine the effect of H_2 pressure on catalytic activity, H_2 pressure was increased from 10 to 30 bar, and the ethylbenzene conversion increased from 52.6% to 100% (Entry 4). In summary, the highest TOF value in the styrene hydrogenation of the PyrNHCH$_2$Bt-Pd catalyst was obtained at 50°C, 30-bar H_2, and 1-ml min^{-1} flow rate conditions (Entry 4).

The efficiency of the PyrNHCH$_2$Bt-Pd catalyst in 1-octene hydrogenation was tested first at low temperature and then at 50°C (Entries 6 and 7). Almost no conversion was observed at both temperatures. When the pressure was gradually increased from 10 to 50 bar at 50°C, the total conversion increased to only 25%. Although *n*-octane selectivity increased when H_2 pressure was increased to 30 and 50 bar values, respectively, the conversion amount remained below 30% (Entries 7–9). It is seen in Table 2 that the most effective parameter in 1-octene hydrogenation is flow rate. When the flow rate was reduced to 0.5 ml min^{-1}, 100% *n*-octane selectivity was obtained (Entry 10).

TABLE 2 Catalytic activity of PyrNHCH$_2$Bt-Pd complex

Substrate	Entry	*T* (°C)	$C_{subst.}$ (M)	Flow rate (ml min^{-1})	H_2 pres. (bar)	Total conv. (%)	Main product (Distrib.%)	TON	TOF
Styrene	1	25	0.1	1	10	21.3	Ethylbenzene	264	3168
	2	25	0.1	0.5	10	22.4	Ethylbenzene	278	1668
	3	50	0.1	1	10	52.6	Ethylbenzene	652	7824
	4	50	0.1	1	30	100	Ethylbenzene	1240	14,880
	5	50	0.5	1	10	35.2	Ethylbenzene	218	2616
1-Octene	6	25	0.1	1	10	0.38	*n*-Octane (0.38%)	4.7	56
	7	50	0.1	1	10	0.3	*n*-Octane (0.13%) 2-Octene (0.17%)	1.6	19
	8	50	0.1	1	30	27.4	*n*-Octane (7.3%) 2-Octene (14.8%) 3-Octene (5.3%)	91	1092
	9	50	0.1	1	50	39.2	*n*-Octane (25.6%) 2-Octene (10.1%) 3-Octene (3.5%)	317	3804
	10	50	0.1	0.5	50	100	*n*-Octane (100%)	1240	7440
	11	50	0.5	0.5	50	98	*n*-Octane (85.7%) 2-Octene (9.1%) 3-Octene (3.2%)	531	3186
Cyclohexene	12	25	0.1	1	10	3.35	Cyclohexane	42	504
	13	50	0.1	1	10	8.45	Cyclohexane	105	1260
	14	50	0.1	1	30	90.4	Cyclohexane	1121	13,452
	15	50	0.1	0.5	30	100	Cyclohexane	1240	7440
	16	50	0.5	0.5	30	96.3	Cyclohexane	597	3582

Note: Residual time is 10 and 5 min for 0.5 and 1-ml min^{-1} flow rates, respectively. $n_{subst} = 0.01$, $n_{cat.} = 7.45 \times 10^{-6}$.

In cyclohexene hydrogenation with PyrNHCH$_2$Bt-Pd complex, the highest TOF value was reached at 50°C, 30-bar H_2 pressure, and 0.5-ml min^{-1} flow rate conditions (Entry 14). As can be seen in Entries 12 and 13 in Table 2, temperature was not very effective on the activity of PyrNHCH$_2$Bt-Pd complex. The most significant effect on the increase in catalytic activity in cyclohexene hydrogenation was obtained when the H_2 pressure was increased from 10 to 30 bar (Entries 13–14). To examine the effect of the flow rate on the catalytic reaction, the flow rate was decreased from 1 to 0.5 ml min^{-1}. Although 100% cyclohexane conversion was achieved at low flow, the TOF value decreased due to the long reaction time (Entry 15).

3.2.3 | Catalytic activity of PyrCOBt-Pd complex

The efficiency of PyrCOBt-Pd catalyst in styrene hydrogenation was found to be higher under milder conditions than the other two complexes. One hundred percent conversion of ethylbenzene was obtained at 25°C, 10-bar H_2 pressure, and 1-ml min^{-1} flow rate (Entry 1 in Table 3).

PyrCOBt-Pd provided 63.7% and 78.2% *n*-octane selectivity for 1-octene hydrogenation at 25°C and 50°C, respectively (Entries 3 and 4). An increase in selectivity was observed when H_2 pressure was increased from 10 to 50 bar at 50°C (Entries 4–6). In these experiments carried out with a flow rate of 1 ml min^{-1}, small amounts of other isomer products besides *n*-octane were detected. The *n*-octane selectivity reached 100% when the flow rate was reduced to 0.5 ml min^{-1} (Entry 7).

It was found that PyrCOBt-Pd catalyst is also very effective in cyclohexene hydrogenation. While the efficiency of the catalyst was low at 25°C, a tremendous increase in activity was observed when the temperature was raised to 50° C (Entries 9 and 10). Although the low flow rate increases the catalytic conversion, the longer the reaction time causes a decrease in the TOF value (Entry 12). Therefore, it can be said that the ideal reaction conditions for the PyrCOBt-Pd complex in cyclohexene hydrogenation are 50°C, 0.1-ml min^{-1} flow

TABLE 3 Catalytic activity of PyrCOBt-Pd complex

Substrate	Entry	*T* (°C)	$C_{subst.}$ (M)	Flow rate (ml min^{-1})	H_2 pres. (bar)	Total conv. (%)	Main product (Distrib.%)	TON	TOF
Styrene	1	25	0.1	1	10	100	Ethylbenzene	1240	14,880
	2	25	0.5	1	10	81.1	Ethylbenzene	503	6036
1-Octene	3	25	0.1	1	10	94	*n*-Octane (63.7%) 2-Octene (20.8%) 3-Octene (9.5%)	790	9480
	4	50	0.1	1	10	99.1	*n*-Octane (78.2%) 2-Octene (15.5%) 3-Octene (5.4%)	970	11,640
	5	50	0.1	1	30	99.8	*n*-Octane (94%) 2-Octene (4.4%) 3-Octene (1.4%)	1166	13,992
	6	50	0.1	1	50	100	*n*-Octane (97.7%) 2-Octene (1.7%) 3-Octene (0.6%)	1211	14,532
	7	50	0.1	0.5	30	100	*n*-Octane (100%)	1240	7440
	8	50	0.5	0.5	30	97.7	*n*-Octane (97.3%) 2-Octene (0.05%) 3-Octene (0.35%)	1211	7266
Cyclohexene	9	25	0.1	1	10	17.1	Cyclohexane	212	2544
	10	50	0.1	1	10	98.1	Cyclohexane	1216	14,592
	11	50	0.1	1	20	99.6	Cyclohexane	1235	14,820
	12	50	0.1	0.5	10	100	Cyclohexane	1240	7440
	13	50	0.5	0.5	10	70.2	Cyclohexane	870	5220

Note: Residual time is 10 and 5 min for 0.5- and 1-ml min^{-1} flow rates, respectively. $n_{subst} = 0.01$, $n_{cat.} = 7.47 \times 10^{-6}$.

rate, and 20-bar H_2 pressure, with the highest TOF value (Entry 11).

Recycling experiments

In the recycling experiments, the system was washed with solvent after each reaction was completed. Washing procedure was carried out until no product and substrate residue were observed in the GC analysis. The cycle experiment was restarted by passing fresh substrate solution through the same catalyst bed. Recycling experiments were performed for 10 cycles under optimal reaction conditions where the efficiency of the catalysts was the highest for each substrate in hydrogenation reactions. As can be seen from Figure 2, all catalysts can be reused in styrene and cyclohexene hydrogenation for 10 cycles without any reduction in their activity. While PyrCOBt catalyst maintained its effectiveness at the end of 10 cycles in 1-octene hydrogenation, 3% and 10% decreases were observed in the activity of PyrBt-Pd and $PyrNHCH_2Bt$-Pd catalysts, respectively.

The optimum reaction conditions in which catalysts have the highest activity are presented in Table 4. It was found that the activities of three catalysts were equal in styrene hydrogenation. When evaluated according to the reaction conditions, it was determined that the PyrCOBt-Pd complex was effective at lower temperature and pressure. The efficiency of $PyrNHCH_2Bt$-Pd catalyst in 1-octene hydrogenation was lower than the other two complexes. In cyclohexene hydrogenation, the efficiency of PyrCOBt-Pd catalysts was found to be higher than other two complexes.

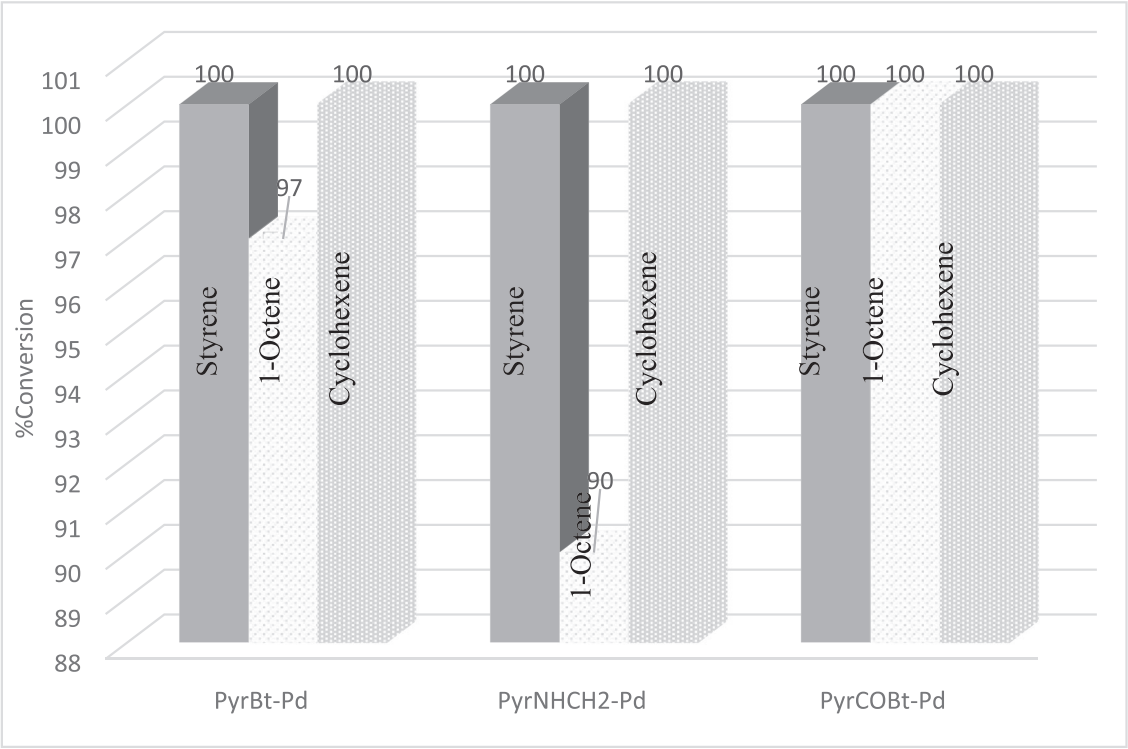

FIGURE 2 Recycling result for 10 cycles

TABLE 4 Optimum reaction conditions in hydrogenation of using substrate

	Styrene				1-Octene				Cyclohexene			
Catalysts	T (°C)	P_{H2} (bar)	Flow rate (ml min^{-1})	TOF	T (°C)	P_{H2} (bar)	Flow rate (ml min^{-1})	TOF	T (°C)	P_{H2} (bar)	Flow rate (ml min^{-1})	TOF
PyrBt-Pd	50	10	1	14,880	50	50	1	**14,880**	50	50	0.5	7440
$PyrNHCH_2Bt$-Pd	50	30	1	14,880	50	50	0.5	7440	50	30	1	13,452
PyrCOBt-Pd	25	10	1	14,880	50	50	1	14,532	50	20	1	14,820

The efficiency of PyrBt-Pd catalyst in styrene hydrogenation was also tested in the high pressure reactor (Parr Inc. 4590 micro Bench Top with 4842 process controller) to compare the continuous flow system and high pressure reactor systems. While 100% ethyl benzene conversion was obtained in 5 min in the continuous flow system at 50°C temperature and 10-bar H_2 pressure, it was determined that the conversion was 96% in 6 h in the high pressure reactor. This result shows that hydrogenation reactions can be carried out in a shorter time and with higher efficiency in the continuous flow system.

4 | CONCLUSION

In this study, we synthesized and characterized three Pd complexes including pyridine-benzotriazole ring that can be used as catalyst. The activity of these complexes as catalyst in olefin hydrogenation reactions was investigated in continuous flow system. It can be concluded that all catalysts have high effectiveness for hydrogenation of using alkenes. When the reaction conditions and TOF values are compared, the efficiency order of the catalysts: PyrCOBt-Pd > PyrBt-Pd = PyrNHCH$_2$Bt-Pd in styrene hydrogenation; PyrBt-Pd > PyrCOBt-Pd > PyrNHCH$_2$Bt-Pd in 1-octene hydrogenation; and PyrCOBt-Pd > PyrNHCH$_2$Bt-Pd > PyrBt-Pd in cyclohexene hydrogenation.

ACKNOWLEDGMENT

This study was supported by Eskişehir Technical University (Project Number: 1701F025).

AUTHOR CONTRIBUTIONS

Filiz Yılmaz: Data curation; formal analysis; investigation; methodology. **Deniz Hür:** Conceptualization; data curation; formal analysis; methodology; project administration.

DATA AVAILABILITY STATEMENT

The data that support the findings of this study are available in the supporting information of this article.

ORCID

Filiz Yılmaz https://orcid.org/0000-0002-6138-0460
Deniz Hür https://orcid.org/0000-0003-0704-1748

REFERENCES

[1] H. A. Patel, M. Rawat, A. L. Patel, A. V. Bedekar, *Appl. Organometal. Chem.* **2019**, *33*, 4767.
[2] M. Keleş, C. Şahinoğlu, D. M. Emir, M. Mart, *Appl. Organometal. Chem.* **2014**, *28*, 768.
[3] E. A. Karakhanov, A. L. Maximov, A. V. Zolotukhina, N. Yatmanova, E. Rosenberg, *Appl. Organometal. Chem.* **2015**, *29*, 777.
[4] G. Vile, N. Almora-Barrios, N. Lopez, J. Perez-Ramirez, *ACS Catal.* **2015**, *5*(6), 3767.
[5] K. Masuda, T. Ichitsuka, N. Koumura, K. Sato, S. Kobayashi, *Tetrahedron* **2018**, *74*, 1705.
[6] W. Bonrath, *Chimia* **2014**, *68*, 485.
[7] R. Ciriminna, M. Pagliaro, *Org. Process Res. Devel.* **2013**, *17*, 1479.
[8] F. Nerozzi, *Platinum Metals Rev.* **2012**, *56*(4), 236.
[9] J. Madarasz, G. Farkas, S. Balogh, A. Szollosy, J. Kovacs, F. Darvas, L. Urge, J. Bakos, *J. Flow Chem.* **2011**, *1*(2), 62.
[10] Y. Wang, P. Prinsen, K. S. Triantafyllidis, S. A. Karakoulia, P. N. Trikalitis, A. Yepez, C. Len, R. Luque, *ACS Sustainable Chem. Eng.* **2018**, *6*(8), 9831.
[11] B. Gutmann, J. P. Roduit, D. Roberge, C. O. Kappe, *Chem. – Eur. J.* **2011**, *17*, 13146.
[12] A. J. Garcia-Olmo, A. Yepez, A. M. Balu, P. Prinsen, A. Garcia, A. Maziere, C. Len, R. Luque, *Tetrahedrom* **2017**, *73*(38), 5599.
[13] T. S. V. R. Neeharika, K. N. P. Rani, K. V. S. A. Rao, T. P. Kumar, R. B. N. Prasad, *Bull. Chem. React. Eng. Catal.* **2013**, *8*(2), 154.
[14] S. Balogh, G. Farkas, J. Madarasz, A. Szollosy, J. Kovacs, F. Darvas, L. Urge, J. Bakos, *Green Chem.* **2012**, *14*, 1146.
[15] Y. Wang, P. Prinsen, K. S. Triantafyllidis, S. A. Karakoulia, A. Yepez, C. Len, R. Luque, *ChemCatChem* **2018**, *10*(16), 3459.
[16] M. Irfan, E. Petricci, T. N. Glasnov, M. Taddei, C. O. Kappe, *Eur. J. Org. Chem.* **2009**, *9*, 1327.
[17] T. Osako, K. Torii, A. Tazawa, Y. Uozumi, *RSC Adv.* **2015**, *5*, 45760.
[18] C. K. Ghosh, A. Chakraborty, *ARKIVOC* **2016**, *2016*(1), 111.
[19] D. Webb, T. F. Jamison, *Chem. Sci.* **2010**, *6*, 675.
[20] T. N. Glasnov, C. O. Kappe, J. Heterocyclic, *Chem* **2011**, *48*, 11.
[21] L. F. Tietze, T. Wolfram, J. J. Holstein, B. Dittrich, *Org. Lett.* **2012**, *14*(16), 4035.
[22] B. Marciniec, Z. Foltynowicz, W. Urbaniak, *Appl. Organometal. Chem.* **1987**, *1*(5), 459.
[23] T. Yu, J. Jiao, P. Song, W. Nie, C. Yi, Q. Zhang, P. Li, *ChemSusChem* **2020**, *13*, 2876.
[24] S. Mhadmhan, A. Franco, A. Pineda, P. Reubroycharoen, R. Luque, *ACS Sustainable Chem. Eng.* **2019**, *7*, 14210.
[25] D. Geier, P. Schmitz, J. Walkowiak, W. Leitner, G. Francik, *ACS Catal.* **2018**, *8*, 3297.
[26] C. Moreno-Marrodana, F. Liguoria, P. Barbaro, H. Sawa, *Appl. Catal. A* **2018**, *558*, 34.
[27] E. Pfab, L. Filiciotto, A. A. Romero, R. Luque, *Ind. Eng. Chem. Res.* **2019**, *58*, 16065.
[28] T. Osako, J. Srisa, K. Torii, G. Hamasaka, Y. Uozumi, *Synlett* **2020**, *31*, 147.
[29] A. K. Rathi, M. B. Gawande, V. Ranc, J. Pechousek, M. Petr, K. Cepe, R. S. Varma, R. Zboril, *Catal. Sci. Technol.* **2016**, *6*, 152.
[30] D. Suna, T. Saitoa, Y. Yamadaa, X. Chenb, S. Sato, *Appl. Catal. A* **2017**, *542*, 289.
[31] T. Chetty, V. D. B. C. Dasireddy, L. H. Callanan, H. B. Friedrich, *ACS Omega* **2018**, *3*, 7911.
[32] D. C. Fabry, S. Heddrich, E. Sugiono, M. A. Liauw, M. Rueping, *React. Chem. Eng.* **2019**, *4*, 1486.

[33] A. R. Katritzky, X. Lan, J. Z. Yang, O. V. Denisko, *Chem. Rev.* **1998**, *98*, 409.
[34] A. R. Katritzky, S. Rachwal, *Chem. Rev.* **2010**, *110*, 1564.
[35] K. A. Mahmoud, I. Slynko, C. Schächtele, F. Totzke, W. Sippl, A. Hilgeroth, *Bioorg. Med. Chem. Lett.* **2014**, *24*(8), 1948.
[36] A. R. Katritzky, B. Pilarski, L. Urogdi, *Org. Prep. Proced. Int.* **1989**, *21*(2), 135.
[37] A. R. Katritzky, K. Suzuki, S. K. Singh, H.-Y. He, *J. Org. Chem.* **2003**, *68*, 5720.
[38] G. Dikmen, D. Hür, *Chem. Phys. Lett.* **2019**, *716*, 49.

SUPPORTING INFORMATION

Additional supporting information may be found online in the Supporting Information section at the end of this article.

How to cite this article: F. Yılmaz, D. Hür, *Appl Organomet Chem* **2021**, e6389. https://doi.org/10.1002/aoc.6389